Pergamon

Int. J. Heat Mass Transfer. Vol. 37, No. 8, pp. 1269–1276, 1994

0017–9310/94 $7.00 + 0.00

0017–9310(93)E00380–I

Condensation of pure vapours and binary vapour mixtures in forced flow

J. KELLENBENZ and E. HAHNE

Institut für Thermodynamik und Wärmetechnik, Universität Stuttgart, Pfaffenwaldring 6, 70550 Stuttgart (Vaihingen), F.R.G.

(*Received* 27 *July* 1992)

Abstract—The coupled processes of heat and mass transfer in film condensation of pure vapours and binary vapour mixtures in forced flow are investigated experimentally. Single-phase resistances for the condensate film and for the vapour flow are determined using the temperature at the vapour/liquid interface. The filmside heat transfer can be represented by identical non-dimensional expressions for pure components and binary mixtures. Using appropriate correction terms for the coupled mass transfer and the roughness of the interface, calculations for pure forced convective heat transfer in the vapour phase show good agreement with the experimental results.

1. INTRODUCTION

FILM CONDENSATION of pure vapours is a purely heat transport problem within the liquid film. This problem was first treated by Nusselt [1] for the limiting case of stagnant vapours. In the case of vapour mixtures the condensation process is a combined problem including coupled heat and mass transfer. In addition to the heat transport resistance in the liquid film there appears another resistance in the vapour phase due to the selectivity of the condensation process. This case was the subject of the work of Colburn and Drew [2], who describe the problem on the basis of the film theory.

In course of condenser design the overall heat transfer resistance has to be calculated. This is usually done using some combination of two single-phase resistances. To obtain these, the temperature and composition at the vapour/liquid interface must be determined considering the coupled processes of heat and mass transfer. The thermodynamic state at the interface is known *a priori* for only two limiting cases: condensation in the thermodynamic equilibrium (with a vanishing rate of condensation) and total condensation (with an extremely large rate of condensation). The problem of evaluating the interfacial conditions is further complicated by the motion of vapour and condensate. Thus heat and mass transfer in the vapour phase may be enhanced by mutual effects of vapour and condensate like momentum transfer, wave formation or entrainment.

There still appear difficulties in calculating such transfer processes, especially in the case of forced vapour flow.

During the condensation process the various parameters such as vapour bulk temperature, wall temperature, vapour composition and condensate mass flux are changing. Therefore only the measurement of local quantities can be used to verify the results of different physical models. In the presented study this concept is followed consequently and the measurement-results may be used as a broad data base on which calculations can be verified.

2. EXPERIMENTAL SETUP

The experimental setup contains a closed loop in which vapour and condensate are circulated. Four additional water loops are used for heating, cooling and temperature control at the entrance of the test section. The experiments are carried out using a vertical test condenser with co-current downward flow of vapour, condensate and cooling water.

2.1. *Test section*

The test section (Fig. 1) consists of two concentric brass tubes with a total length L_{tot} of 2.17 m. Inside diameter and wall thickness of the inner tube are $d = 31$ mm and $s = 9.9$ mm, respectively. Both the inner and outer tube form an annulus which is divided into two parts by a ring shaped movable piston. The active length of the condenser is identical with the water cooled section below the piston whereas condensation above the piston is avoided by hot water circulating in the upper part with a temperature slightly above vapour inlet temperature. The position of the piston can be varied in eight steps of 0.25 m in order to obtain a cooled length in the range $0.134 \leqslant L \leqslant 2.134$ m.

2.2. *Measurement technique*

The experiments are focused on the direct determination of local quantities. In order to achieve this, a cylindrical probe made of stainless steel is installed near the end of the test section (see Fig. 1). The probe contains six thermocouples on the inner perimeter and three thermocouples on the outer

NOMENCLATURE

a	thermal diffusivity [$m^2 s^{-1}$]
A, B	correlation parameters in equation (4)
c_p	specific heat capacity [$J kg^{-1} K^{-1}$]
d	tube diameter [m]
g	gravitational acceleration [$m s^{-2}$]
L	active condenser length [m]
m_c	condensation flux [$kg m^{-2} s^{-1}$]
Nu_f	Nusselt number of the film, $\alpha_f(\nu_f^2/g)^{1/3}/\lambda_f$
Nu_v	Nusselt number of the vapour, $\alpha_v d/\lambda_v$
Pr	Prandtl number, ν/a
q	heat flux [$W m^{-2}$]
R	heat transport resistance [$m^2 K W^{-1}$]
Re_f	Reynolds number of the film, $u_f\delta/\nu_f$
Re_v	Reynolds number of the vapour, $Re_v = u_v d/\nu_v$
s	wall thickness [m]
T	temperature [K]
u	velocity [$m s^{-1}$]
y	mole fraction (more volatile component) in the vapour phase.

Greek symbols

α	heat transfer coefficient [$W m^{-2} K^{-1}$]
δ	thickness of condensate film [m]
λ	thermal conductivity [$W m^{-1} K^{-1}$]
ν	kinematic viscosity [$m^2 s^{-1}$]
ξ	friction factor
ρ	density [$kg m^{-3}$]
τ	shear stress [$N m^{-2}$]
τ^*	non-dimensional shear stress, $\tau/(g\rho_f\delta)$
Φ_T	rate factor, temperature profile
Φ_v	rate factor, velocity profile
Ψ_m	correction factor according to coupled heat and mass transfer
Ψ_r	correction factor according to vapour/liquid interactions
Ω	velocity ratio (equation 6).

Subscripts

b	bulk
f	film
i	interface vapour/liquid
in	inlet
m	with respect to mass transfer
mix	mixture
o	outside
ov	overall
pc	phase change
r	with respect to rough surfaces
s	with respect to smooth surfaces
sat	saturation
sup	superheating
tot	total
v	vapour
wi	wall inside
wo	wall outside
1ph	single-phase flow
2ph	two-phase flow.

Superscript

•	with respect to coupled mass transfer.

perimeter. This allows the measurement of the local heat flux. Another thermocouple is located in the axis of the tube (in the centre of the probe) for measuring the vapour bulk temperature.

Additional temperature measurements include vapour at the inlet and outlet, condensate at the outlet and temperature rise of the cooling water. All temperatures are measured with calibrated Chromel/Alumel thermocouples. The mass flux of vapour is measured with rotameters. The condensate is collected periodically in a calibrated measurement cylinder made of glass to determine the mass flux. The vapour compositions are measured with a gas chromatograph (GC) while the composition of the condensate is determined continuously with a refractometer and checked by analysing liquid samples with the GC. In addition the pressure in the test section is measured with a piezoresistive pressure transducer.

2.3. *Test fluids and experimental parameters*

As test fluids the two refrigerants R11 (trichlorofluoromethane CCl_3F) and R113 (trichlorotrifluoroethane $C_2Cl_3F_3$) are investigated. The physical properties of the pure substances were used according to the manufacturer's informations [3, 4]. The binary mixture R11/R113 shows ideal mixing behaviour [5]. In lack of measurements the properties of the mixture were calculated following the recommendations in literature [6].

During the experiments the following parameters were varied systematically:

- active condenser length
  (4 steps with $L = 0.6; 1.1; 1.6; 2.1$ m)
- temperature difference between vapour and cooling water (inlet)
  ($\Delta T = 7$ and 14 K)
- Reynolds number of the vapour (inlet)
  ($Re_{v,in} = 60\,000, 140\,000, 170\,000$)
- mole fraction of R11 in the vapour phase (inlet)
  ($y_{in} = 0, 0.1, 0.3, 0.5, 0.7, 0.9, 1.0$).

This set of parameters allows for local heat fluxes at the bottom of the test section of $2600 \leqslant q \leqslant 8100$

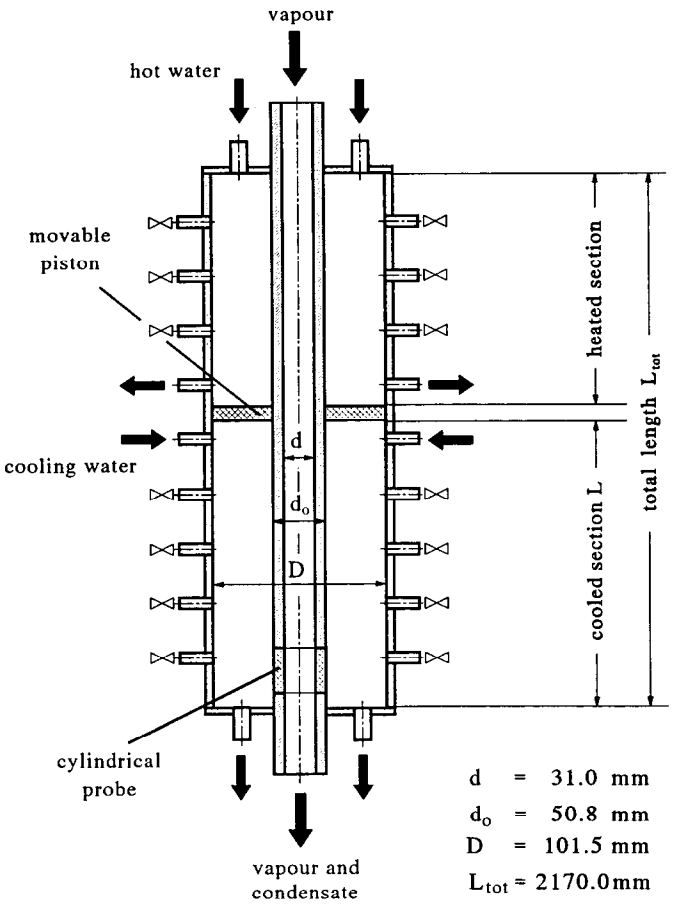

FIG. 1. Test section.

W m^{-2} and film Reynolds numbers of $20 \leqslant Re_f \leqslant 200$ which is in the laminar and laminar-wavy flow regime.

3. EVALUATION

The temperature profile in a cross-section of the condenser is used to give exact definitions of the different heat transfer coefficients (see Fig. 2). First the temperature profile for condensation of pure vapours is explained to emphasize the differences concerning the more complicated case in condensation of binary vapour mixtures.

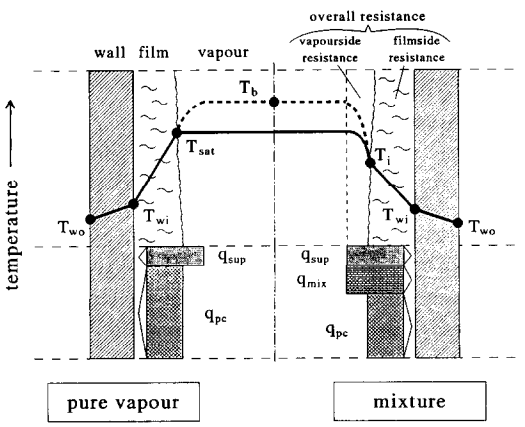

FIG. 2. Temperature distribution in condensation of pure vapours and binary vapour mixtures.

At constant pressure a condensing pure vapour has a fixed temperature, i.e. the saturation temperature. If the inlet vapour flow is superheated a temperature profile is obtained between T_b in the bulk and T_{sat} at the interface. This temperature difference is reduced throughout the condenser and can usually be neglected. The corresponding heat flux from superheating (q_{sup}) is smaller by orders of magnitude than the heat flux arising at the vapour/liquid interface due to the phase change (q_{pc}). As a result only a single heat transfer resistance in the liquid film has to be regarded. This is the case treated by Nusselt [1]. The most important difference between condensation of pure vapours and vapour mixtures is the existence of an additional heat transfer resistance in the latter case. This resistance is a consequence of the preferred condensation of the less volatile component. In the same manner as the concentration of the less volatile component decreases within a small vapour layer adjacent to the liquid film, the saturation temperature of the vapour mixture also decreases. This temperature profile is maintained throughout the condenser, since it

is a consequence of the condensation process itself. In the case of mixtures there may also be an additional temperature drop due to superheating of the vapour. Regarding the heat fluxes, still most of the total heat flux is arising at the interface q_{pc}, again supplemented by a small amount of q_{sup}, but there remains an additional heat flux q_{mix} from the temperature drop in the vapour layer, even if the vapour bulk is at saturation state. These facts have to be considered in defining heat transfer coefficients.

The temperature of the vapour/liquid interface T_i is the key for an evaluation of separate heat transfer coefficients in vapour and liquid phase. No technique is available for the direct measurement of this temperature with sufficient accuracy. Therefore T_i has to be determined from other directly measured quantities by applying certain assumptions, e.g. concerning the concentration profile inside the condensate film. For the present evaluation two assumptions were made: (i) a completely mixed film with (ii) thermodynamic equilibrium at the interface. T_i is evaluated from the measured condensate composition using the vapour/liquid phase equilibrium given by [5].

The maximum error caused by the first assumption (i) (the latter assumption (ii) is very common) was estimated in simulation calculations supposing the contrary behaviour of a completely unmixed, i.e. stratified, film as a limiting case. The error is dominated by the selectivity of the condensation process (difference in composition of vapour and condensate) and the extent of the condensation process (ratio of mass fluxes of condensate and vapour at the outlet). For the range of parameters investigated here the maximum error is 0.8 K, the minimum error is 0.01 K. It must be emphasized that these calculated errors are upper limits of the actual error due to the unrealistic assumption of an unmixed film. The measurement technique used here leads to a maximum additional error of 0.15 K. The results of the calculations may be used to define limiting ranges in which the maximum error of T_i is small.

For the definition of the following heat transfer coefficients the superheating of vapour is neglected ($T_b \approx T_{sat} \rightarrow q_{sup} \approx 0$).

(i) The overall heat transfer coefficient defined by

$$\alpha_{ov} = \frac{q_{tot}}{T_{sat} - T_{wi}} \tag{1a}$$

resulting in the overall resistance

$$R_{ov} = \frac{1}{\alpha_{ov}} = \frac{T_{sat} - T_{wi}}{q_{tot}} \tag{1b}$$

summarizes the resistances in the condensate film (filmside resistance) and the vapour phase (vapourside resistance). There is no direct physical meaning since the total heat flux is related to a temperature difference, which is not the driving potential for this flux (the phase change at the interface acts as a heat source). As already mentioned it is necessary to split this overall heat transport resistance into single-phase resistances.

(ii) The heat transfer coefficient for the condensate film is

$$\alpha_f = \frac{1}{R_f} = \frac{q_{tot}}{T_i - T_{wi}} \tag{2}$$

this equals α_{ov} in the case of a pure condensing vapour (with $T_i = T_{sat}$). For mixtures the ratio α_{ov}/α_f is a quantity for the portion of the driving potential across the film ($T_i - T_{wi}$) compared to the total potential ($T_{sat} - T_{wi}$) or in other words the fraction of the overall resistance which is caused by the condensate film. In all experiments reported here the reduction of α_{ov} in the case of vapour mixtures compared to α_f does not exceed 30%, i.e. the filmside resistance causes at least 70% of the overall resistance.

For the flow conditions investigated here (turbulent vapour flow—laminar film flow) the domination of the film resistance will continue to exist even in the case of other mixtures with a greater difference in boiling temperatures. Therefore the disadvantageous influence of an additional vapourside resistance is not so pronounced.

(iii) Finally the vapourside heat transfer coefficient is expressed as

$$\alpha_v = \frac{1}{R_v} = \frac{q_{mix}}{T_{sat} - T_i}. \tag{3}$$

Using the different heat transfer coefficients, Nusselt numbers can be defined similarly.

4. RESULTS AND DISCUSSION

4.1. *Heat transfer—condensate film*

Pure vapours. Figure 3 shows the results for both investigated fluids. The Nusselt number Nu_f for the film is plotted versus the film Reynolds number Re_f in double logarithmic scale for three different vapour Reynolds numbers $Re_{v,in}$ at the inlet.

The results for both fluids compare within $\pm 10\%$ for a given Reynolds number $Re_{v,in}$ with a mean deviation of 4%. The data of both fluids (R113, R11) can be correlated by

$$Nu_f = A \cdot Re_f^B \quad (A, B = f(Re_{v,in})). \tag{4}$$

The parameters A and B obtained by r.m.s. fit of equation (4) are listed in Table 1. The respective curves are given in Fig. 3 as dashed and dashed–dotted lines.

For comparison Fig. 3 includes two solid lines, one calculated from Nusselt's theory [1] and another from the empirical correlation by Dialer [7] regarding the waviness of the liquid film. Both are valid for stagnant vapour. The experimental results for the lowest Reynolds number ($Re_{v,in} = 60\,000$) agree very well with Dialer's correlation. This can be explained if the non-dimensional shear stress τ^* at the vapour/liquid interface is considered. The shear stress τ^* is the ratio

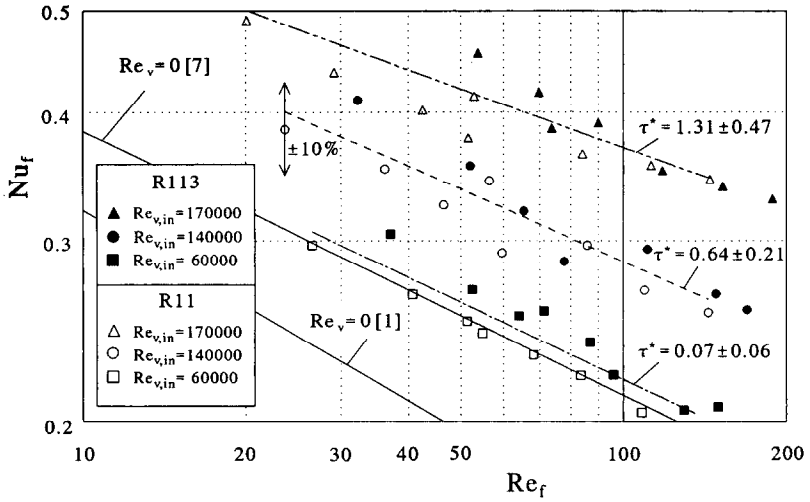

FIG. 3. Correlation of the Nusselt number Nu_f with the Reynolds number of the film for pure vapours of R11 and R113 (τ^* non-dimensional shear stress).

of the friction force at the interface due to the vapour flow and the gravity force of the liquid film. The calculation of τ^* for vertical annular flow is based on the model of Asali *et al.* [8] using the modifications presented in ref. [9]. For the lowest $Re_{v,in}$ number $\tau^* \approx 0.07$ which is close to zero. Thus the film thickness (i.e. the heat transfer resistance) is governed by gravity and the thinning effect due to the shear stress vanishes. The thinning effect of the shear stress, on the other hand, becomes more pronounced when the Re_v number is increased. This yields a strong enhancement of the Nu_f number at a given Re_f number. The fitted curves are shifted almost in parallel.

Vapour mixtures. In the case of vapour mixtures two heat transfer coefficients (α_f and α_v) have to be considered. For the evaluation of the respective Nusselt and Reynolds numbers (Nu_f, Nu_v, Re_f, Re_v) the physical properties of the actual mixture are required. The filmside results are plotted in Fig. 4 for various vapour mixtures. A detailed evaluation of the experimental error is used to include only those measurements with a tolerable accuracy. This was achieved using the sum of the average error (for all measurements) and the respective standard deviation as an upper limit.

The scatter of data points is more pronounced than in the case of pure vapours but nevertheless they can be represented within ±20% (with the exception of two points) and a mean deviation of 6.6% by the correlations for *pure vapours* (see dashed lines as transferred from Fig. 3).

Table 1. Correlation parameters according to equation (4)

Re_v	A	B
60000	0.6933	−0.2492
140000	0.8360	−0.2326
170000	0.8843	−0.1896

The data in Fig. 4 are obtained for mole fractions of R11 at the inlet ranging from 0.1 to 0.9. A systematic distribution of these fractions cannot be observed which means that there is no effect of composition. Thus the non-dimensional heat transfer resistance of a laminar liquid film can be predicted by a unique expression (equation (4)) for either liquid and liquid mixture used here (for constant interfacial shear stress). This has already been mentioned by other investigators (e.g Onda *et al.* [10]).

4.2. *Heat transfer—vapour phase*

The vapourside heat transfer resistance vanishes for a pure condensing vapour without superheating. However, it becomes important if the condensation of a vapour mixture is considered. In this case the heat transfer is influenced by various physical processes. The first question is directed to the vapour flow pattern in the bulk. In all experiments presented, the vapour flow was highly turbulent with Reynolds numbers at the outlet of $25000 < Re_v < 170000$. Condensation of vapour mixtures is a problem which involves the coupled transport processes of heat, mass and momentum. The transport processes may either be considered to occur within the total vapourside cross-section, or they may be reduced to the laminar sublayer as suggested by the so called 'film theory'. In both cases heat transfer is affected by mass and momentum transfer normal to the vapour main flow, i.e. in radial direction. Finally there are interactions between condensate and vapour flow that may increase the heat transfer due to wave formation, etc.

In the following sections the experimental results are compared with semi-empirical relations taking into account these physical processes step by step. Again the data with a maximum error larger than the sum of the average error and the respective standard deviation were excluded.

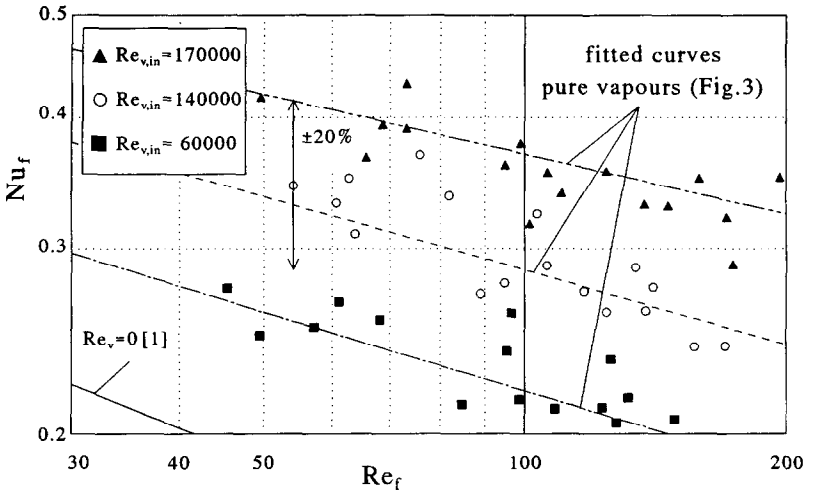

FIG. 4. Correlation of the Nusselt number Nu_f with the Reynolds number of the film for binary mixtures (y_{in} = 0.1; 0.3; 0.5; 0.7; 0.9 mole fraction R11).

Starting with an appropriate correlation for convective heat transfer in single-phase turbulent flow, two correction factors (Ψ_r, Ψ_m) for the considered heat transport problem will be derived. Based on the Prandtl analogy:

$$Nu_{v,1ph} = \frac{\xi_s}{8} Re_v\, Pr_v \frac{1}{1+\Omega(Pr_v-1)} \tag{5}$$

—with ξ_s as the friction factor calculated for a smooth tube and Ω as the ratio between maximum and average velocities—Nunner [11] developed a theory for the prediction of heat transfer in rough tubes (without superimposed mass transfer).

Nunner's extension of the Prandtl analogy leads to the following equation:

$$Nu_{v,1ph} = \frac{\xi_r}{8} Re_v\, Pr_v \frac{1}{1+\Omega(Pr_v\,\xi_r/\xi_s-1)} \tag{6}$$

where ξ_r is the fraction factor for rough surfaces and Ω is a velocity ratio that has to be determined experimentally. As shown by Nunner [11] Ω is almost independent of the roughness. Therefore empirical Ω-correlations determined in smooth tubes may be used even in the case of rough surfaces.

As a consequence of the velocity difference between vapour and condensate there arises a shear stress at the vapour/liquid interface. This shear stress results in a flow dependent deformation of the film which is no longer smooth. The friction factor ξ_r for the wavy film exceeds the respective factor ξ_s for a smooth surface and so do the heat and mass transfer coefficients. As shown by several investigators the individual characteristics of the roughness are of less importance. Therefore Nunner's theory may be used even in the case of an annular two-phase flow with a wavy, i.e. rough, condensate film.

The empirical correlation (equation (7)) by Gnielinski [12], which is an excellent representation of experimental results for convective heat transfer in turbulent flow, is also based on the Prandtl analogy:

$$Nu_{v,1ph} = \frac{\xi_s}{8}(Re_v-1000)Pr_v[1+1/3(d/L)^{2/3}] \times \frac{1}{1+12.7\sqrt{(\xi_s)}(Pr_v^{2/3}-1)} \tag{7}$$

$$\xi_s = (1.82\log Re_v - 1.64)^{-2}.$$

This gives rise to the idea of applying the results of Nunner's theory to equation (7) where $\xi_s/8$ and (Pr_v-1) are replaced by $\xi_r/8$ and $(Pr_v\,\xi_r/\xi_s-1)$, respectively, and maintaining Ω.

As an additional effect of the condensation process the cross-sectional velocity profile is distorted by the mass transfer. The film theory [13] provides a simple correlation for the enhancement of the friction factor due to coupled momentum and mass transfer:

$$\frac{\xi_r^\bullet}{\xi_r} = \frac{\Phi_v}{(1-\exp(-\Phi_v))} \quad \text{with} \quad \Phi_v = \frac{m_c u_c}{\tau_r}. \tag{8}$$

The consequent application of these correction factors leads to the following modification of equation (7):

$$Nu_{v,2ph} = \frac{\xi_r^\bullet}{8}(Re_v-1000)Pr_v[1+1/3(d/L)^{2/3}] \times \frac{1}{1+\Omega(Pr_v\,\xi_r^\bullet/\xi_s-1)} \tag{9}$$

$$\Omega = \frac{(Pr_v^{2/3}-1)}{(Pr_v-1)}12.7\sqrt{(\xi_s/8)}$$

$$\xi_s = (1.82\log Re_v - 1.64)^{-2}.$$

This procedure was successfully applied by Numrich [14] in partial condensation of steam–air mixtures using a Ω-correlation slightly different from equation (9).

Comparing equations (7) and (9) a correction

factor (exclusively for the interaction of vapour flow and condensate film) Ψ_r is defined by the following equation:

$$\Psi_r = Nu_{v,2ph}/Nu_{v,1ph}. \quad (10)$$

From equation (9) it can be concluded that Ω is of minor importance when Pr_v is close to unity (for most gases). In this investigation Pr_v is within $0.819 < Pr_v < 0.850$ with a mean value of $Pr_v = 0.835$. Therefore the ratio ξ_r^*/ξ_s is a good approximation for the correction factor Ψ_r but nevertheless the exact value of Ψ_r is used throughout this work.

Finally the calculation of the correction factor Ψ_r reduces to the problem of correct determination of the friction factor ξ_r and the shear stress τ_r for rough surfaces. Again the model of Asali *et al.* [8] using the modifications presented in ref. [9] is used to calculate ξ_r. Beside the physical properties, only the Reynolds numbers Re_f and Re_v are input parameters for this model.

In the case of coupled heat and mass transfer there arises an additional heat transfer mechanism. This is a consequence of the condensing mass flux which transports energy from a region with high temperature (vapour bulk) to a region with low temperature (interface). In the present work the film theory is used to describe this problem. This leads to simple correction factors [13] also known as Ackermann correction Ψ_m:

$$\Psi_m = \frac{\Phi_T}{(1-\exp(-\Phi_T))} \quad \text{with} \quad \Phi_T = \frac{m_c c_{pv}}{\alpha_{v,2ph}}. \quad (11)$$

It should be emphasized that in agreement with the assumption of the film theory the enhanced value $\alpha_{v,2ph}$ for heat transfer in two-phase flow (calculated from equation (9)) has to be used throughout equation (11).

Thus the correction factor concerning coupled heat and mass transfer is identical with the Ackermann correction Ψ_m:

$$\Psi_m = Nu^*_{v,2ph}/Nu_{v,2ph}. \quad (12)$$

In order to get a unified representation of data, the values of the experimental Nusselt number were divided by the total correction factor $(\Psi_m \cdot \Psi_r)$. Following the theory derived here, these modified values labelled as $Nu_{v,mod}$ should coincide with the correlation, equation (7), by Gnielinski [12].

The result with Ψ_m and Ψ_r ranging from $1.02 \leqslant \Psi_m \leqslant 1.40$ and $1.08 \leqslant \Psi_r \leqslant 1.53$, respectively, is shown in Figure 5. The corrected data are in agreement with equation (7) within $\pm 25\%$ uncertainty bounds.

In the case of *small* Re_v, i.e. small heat transfer coefficients, the influence of coupled heat and mass transfer is significant but it is also affected by the condensing mass flux m_c. Here Ψ_m reaches the maximum value of 1.40. In this region the heat transfer is hardly influenced by the interactions of vapour and film flow. For those flow conditions the deformation and acceleration of the film due to the shear stress at the interface is only small. This is in agreement with the experimental results for the condensate film. For small $Re_{v,in}$ the heat transfer conditions in the liquid film proved to be very close to the case of stagnant vapour (see Section 4.1).

In the case of *large* Re_v and large Re_f the value of Ψ_r reaches its maximum of 1.53. Here the influence of the interaction of vapour and condensate Ψ_r predominates the coupling effect of heat and mass transfer Ψ_m.

5. CONCLUSIONS

The non-dimensional representation of the heat transfer across condensate films can be correlated with Re_f and $Re_{v,in}$ numbers using identical expressions for

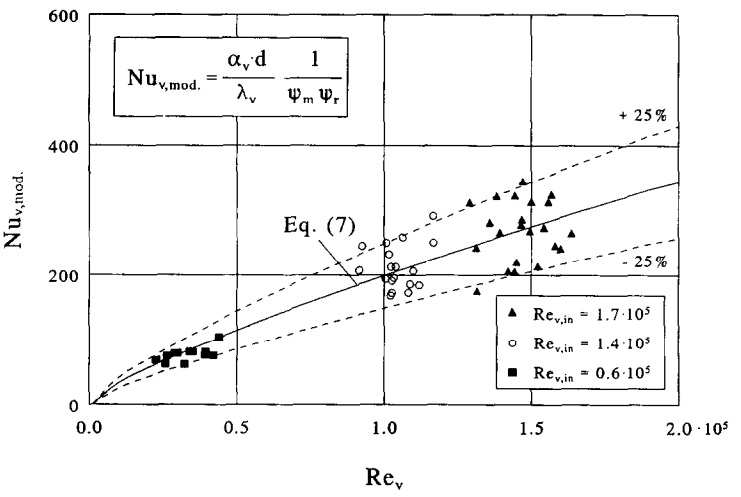

FIG. 5. Representation of the experimental data concerning the total correction for coupled heat and mass transfer and vapour/liquid interactions.

various fluids and fluid mixtures. This holds even in the case of turbulent vapour flow. The correlation for $Re_{v,in} = 60\,000$ agress very well with relations from literature for stagnant vapour. Concerning the experimental values, the increase in vapour mass flux yields an increase of the interfacial shear stress up to $\tau^* \approx 1.3$ and by this an enhancement of heat transfer coefficients up to 60% compared to the case of stagnant vapour.

The heat transfer in the vapour phase is influenced by the actual flow conditions in the vapour bulk, the superimposed mass transfer and the interaction of vapour flow and condensate film. Using appropriate semi-empirical correction factors to describe these physical processes, the experimental data are predicted correctly within $\pm 25\%$. In the case of small Re_v the effect of mass transfer on heat transfer is more pronounced whereas the interaction of vapour and condensate predominates in the region of large Re_v.

For the investigated flow conditions (turbulent vapour flow—laminar film flow) the film resistance reaches about 70% of the total resistance. Therefore the disadvantageous influence of an additional heat transfer resistance in the case of binary vapour mixtures is comparatively small. By increasing the vapour mass flux both the vapourside and the filmside resistances are reduced and the performance of the condenser is improved considerably.

Acknowledgement—This research was made possible by grants of the Deutsche Forschungsgemeinschaft (DFG) which is gratefully acknowledged by the authors.

REFERENCES

1. W. Nusselt, Die Oberflächenkondensation des Wasserdampfes, *Zeitschrift VDI Band* **60**(27), 541–575 (1916).
2. A. P. Colburn and T. B. Drew, The condensation of mixed vapours, *A.I.Ch.E. Trans.* **33**, 197–215 (1937).
3. R. Döring, *Kaltron 11—Thermodynamische Eigenschaften*. Kali-Chemie AG, Hannover.
4. R. Döring, *Kaltron 113—Thermodynamische Eigenschaften*. Kali-Chemie AG, Hannover.
5. J. Fink, Verdampfung von R11/R113-Gemischen an einem quer angeströmten waagrechten Zylinder, Diss. Universität Clausthal-Zellerfeld (1982).
6. R. C. Reid, J. M. Prausnitz and T. K. Sherwood, *The Properties of Gases and Liquids* (4th Edn). McGraw-Hill, New York (1988).
7. K. Dialer, Neue Gleichungen für den Wärmeübergang an senkrechten Kondensatorrohren, *Swiss Chem.* **4**(10a), 19–23 (1982).
8. J. C. Asali, T. J. Hanratty and P. Andreussi, Interfacial drag and film height for vartical annular flow, *A.I.Ch.E. Jl* **31**(6), 895–902 (1985).
9. *VDI-Wärmeatlas* (5th Edn). Verlag, Düsseldorf (1988).
10. K. Onda, E. Sada and K. Takahashi, The film condensation of mixed vapour in a vertical column, *Int. J. Heat Mass Transfer* **13**, 1415–1424 (1970).
11. W. Nunner, Wärmeübergang und Druckverlust in rauhen Rohren. VDI-Forschungsheft 455 (1956).
12. V. Gnielinski, Neue Gleichungen für den Wärme- und Stoffübergang in turbulent durchströmten Rohren und Kanälen, *Forsch. Ing.-Wes.* **41**(1), 8–16 (1975).
13. R. B. Bird, W. B. Stewart and E. N. Lightfoot, *Transport Phenomena*. Wiley, New York (1960).
14. R. Numrich, Die partielle Kondensation eines Wasserdampf/Luftgemisches im senkrechten Rohr bei Drücken bis 21 bar. VDI-Fortschrittsberichte Reihe 3, Nr 165 (1988).